Applied Chemical Engineering (2026) Volume 9 Issue 1 ISSN: 2578-2010 (O)
doi: 10.59429/ace.v9i1.5772

ORIGINAL RESEARCH ARTICLE

Electronic, Optical, Vibrational, and Interaction Properties of Gefitinib and Quercetin: An Integrated DFT and Docking Study with Relevance to Applied Chemical Engineering

Ali Hayder Hamzah[1], Hussein Odia[2], Hamed A. Gatea[3], Maithm A. Obaid[3], Alzahraa S. Abdulwahid[4], Hadil Hussain Hamza[5], Mohannad Abdulrazzaq Gati[6], Aseel M. aljeboree[7], Ayad F. Alkaim*[7,] Ali Aqeel Mahmood[8]

[1] *College of Pharmacy, Al-Turath University, Baghdad, Iraq, 10012, Iraq,*

[2] *Medical Technical College, Al-Farahidi University, Baghdad, Iraq.*

[3] *College of Applied Medical Science, Shatrah University, Thi-Qar, 64001, Iraq*

[4] *College of Pharmacy, Al-Hadi University College, Baghdad,10011, Iraq,*

[5] *Department of Medical Laboratories Technology, Al-Nisour University College, Nisour Seq. Karkh, Baghdad, 10012,Iraq*

[6] *College of Health and Medical Technologies, National University of Science and Technology, Dhi Qar, 64001,Iraq*

[7] *Department of chemistry, College of science for women, University of Babylon, Hilla, 5001, Iraq.*

[8] *College of Health and Medical Techniques, AL-Bayan University, Baghdad, Iraq*

***Corresponding author:** Ayad F. Alkaim alkaimayad@gmail.com

ARTICLE INFO

Received: 18 September 2025
Accepted: 06 December 2025
Available online: 31 December 2025

ABSTRACT

We present a computational investigation of Gefitinib, a clinically approved EGFR inhibitor, and Quercetin, a bioactive flavonoid with anticancer potential, through an integrated density functional theory (DFT), time-dependent DFT (TD-DFT), and molecular docking framework. Geometry optimization at the B3LYP/6-31G(d,p) level yielded electronic and global reactivity descriptors, providing insights into molecular stability and interaction potential. Quercetin exhibited higher electronic stability, with a HOMO–LUMO gap of 5.22 eV compared to 4.24 eV for Gefitinib. TD-DFT simulations predicted key absorption bands at ~369 nm for Gefitinib and ~310 nm for Quercetin, correlating with their distinct electronic transitions. Docking studies against the EGFR tyrosine kinase domain (PDB: 4HJO) revealed stronger predicted binding for Quercetin (−8.9 kcal/mol) than Gefitinib (−5.5 kcal/mol), supported by hydrogen bonding and π–π stacking interactions. These findings highlight how computational chemistry techniques, widely applied in materials design and process optimization, can also provide multiscale insights into drug–target interactions. By integrating electronic structure analysis with molecular docking, this study demonstrates a transferable approach relevant to applied chemical engineering, bridging quantum chemistry with molecular interaction studies in pharmaceutical and materials science contexts.

Keywords: DFT; TD-DFT; Molecular Docking; Gefitinib; Quercetin; Interaction Properties; Applied Chemical Engineering

1. Introduction

Lung cancer remains one of the most fatal malignancies worldwide, with non-small cell lung cancer (NSCLC) accounting for nearly 85% of reported cases, and mutations in the epidermal growth factor receptor (EGFR) are a central driver of tumorigenesis and therapeutic resistance [1-3]. Conventional therapeutic strategies have leveraged tyrosine kinase inhibitors (TKIs), among which Gefitinib, a first-generation EGFR inhibitor, gained FDA approval for NSCLC therapy due to its ability to target the ATP-binding pocket of EGFR. However, despite initial clinical efficacy, challenges such as acquired resistance (e.g., T790M mutations), off-target toxicity, and limited long-term survival outcomes reduce the overall therapeutic benefits of Gefitinib [4-6]. These limitations have encouraged researchers to investigate combinatorial or alternative therapeutic candidates, with naturally derived bioactive molecules receiving increasing attention. Quercetin, a dietary flavonoid found in fruits and vegetables, has emerged as a promising candidate due to its well-documented antioxidant, anti-inflammatory, and anticancer properties [7-9] . Computational studies and experimental cell-based assays have indicated that Quercetin can interact with EGFR, thereby modulating oncogenic pathways and potentially delaying resistance mechanisms that undermine Gefitinib monotherapy [10-12]. In this context, it becomes necessary to employ advanced computational approaches to systematically evaluate and compare the electronic, optical, vibrational, and interaction properties of these molecules, thereby offering predictive insight into their therapeutic potential.

The challenges surrounding the rational design of therapeutic agents bear strong resemblance to materials selection and process optimization problems in applied chemical engineering, where molecular-level descriptors and performance indices are used to optimize macroscopic properties of polymers, composites, and engineered surfaces. For example, decision-making models for composite polymers [13], infill pattern optimization for thermoplastic polyurethane in pipelines [14], and surface property control in additive manufacturing [15,16] demonstrate that computational optimization principles are widely transferable across disciplines. Similarly, the need to understand and tune electronic descriptors such as frontier molecular orbitals (HOMO–LUMO), reactivity indices, and electrostatic potentials parallels studies in biopolymer sustainability and nanocomposite surface engineering [17,18]. In drug discovery, these descriptors are crucial to understanding molecular stability, reactivity, and biological binding interactions, while in chemical engineering they underpin material stability, adsorption, catalysis, and surface modification. Recent advances in bio-based polymer optimization [19, 20], surface metamorphosis of polymers [21], and catalytic coatings in fused deposition modeling [22] highlight the broader applicability of computational workflows, bridging molecular chemistry with applied engineering contexts.

The state of the art in computational chemistry for drug discovery typically involves density functional theory (DFT) for structural optimization, vibrational analysis, and reactivity descriptors, alongside time-dependent DFT (TD-DFT) for optical excitations and density of states (DOS) analysis. These techniques have long been applied in materials chemistry, catalysis, and nanotechnology to optimize molecular-level features that influence macroscopic engineering performance. For instance, DFT studies on polymeric nanocomposites have been widely reported for predicting adsorption, surface energy, and mechanical reinforcement [23, 24], while in the pharmaceutical field, they provide predictive insights into stability and drug–target interactions. Similarly, optimization techniques in additive manufacturing have utilized computational and experimental synergies to enhance process efficiency and surface morphology [25,26]. This convergence of methods highlights the versatility of DFT and related computational tools in solving both drug design and chemical engineering problems, underscoring the importance of cross-disciplinary frameworks. Despite such advances, few studies integrate a multiscale analysis of synthetic drugs and natural compounds from electronic structure to molecular docking within the same systematic framework. Bridging this gap not only advances rational drug design but also demonstrates the wider relevance of computational methodologies in applied chemical engineering domains, where optimization, sustainability, and interaction analysis are key drivers.

Against this background, the present study conducts a comprehensive computational investigation of Gefitinib and Quercetin, employing DFT-based geometry optimization, vibrational frequency analysis, frontier molecular orbital mapping, and global reactivity descriptors to elucidate their inherent stability and electronic behavior. Time-dependent DFT calculations further allow prediction of UV–Vis spectra and optical transitions, while density of states analysis provides insight into orbital contributions and energy distributions [27-29]. These quantum chemical descriptors are coupled with molecular docking simulations against the EGFR tyrosine kinase domain (PDB: 4HJO) to evaluate drug–target binding affinities, hydrogen bonding networks, and non-covalent interactions. By systematically comparing a synthetic EGFR inhibitor (Gefitinib) with a natural flavonoid (Quercetin), this work not only evaluates the potential of Quercetin as a complementary or alternative therapeutic candidate but also illustrates how computational frameworks widely used in chemical engineering for materials optimization can be adapted to pharmaceutical design [30-32]. The novelty of this study lies in its integrated approach: combining electronic structure theory, optical analysis, density of states, and protein–ligand docking into a single multiscale workflow that can be generalized beyond pharmaceuticals to applied chemical engineering systems, such as sustainable polymer design, catalytic surface interactions, and nanocomposite optimization [33-35]. By doing so, this research not only addresses the pressing challenge of drug resistance in cancer therapy but also demonstrates the methodological convergence between computational chemistry and applied chemical engineering, offering a platform for future cross-disciplinary innovations.

2. Materials and methods

The computational methodology adopted in this work was designed to provide an integrated understanding of the structural, electronic, vibrational, optical, and interaction properties of Gefitinib and Quercetin, with procedures aligned to established protocols in quantum chemistry and adapted concepts from chemical engineering optimization frameworks. Initially, the molecular structures of Gefitinib and Quercetin were obtained from the PubChem database in SDF format and subsequently converted to Gaussian input files using GaussView 6.0. Structural optimization was performed in the gas phase using Density Functional Theory (DFT) at the B3LYP/6-31G(d,p) level, implemented in Gaussian 09, and confirmed as true minima on the potential energy surface by frequency analysis showing no imaginary vibrational frequencies. This choice of basis set and functional is widely accepted in both pharmaceutical modeling and materials chemistry applications, ensuring a balance between computational efficiency and accuracy in predicting ground-state properties [36-37]. In parallel, methodological parallels can be drawn with optimization workflows in additive manufacturing and sustainable polymer development, where computational design and multi-criteria decision-making models are utilized for material selection and parameter optimization [38-40]. Following geometry optimization, the frontier molecular orbital (FMO) energies, namely the highest occupied molecular orbital (HOMO) and lowest unoccupied molecular orbital (LUMO), were extracted to compute global reactivity descriptors including electronegativity (χ), chemical hardness (η), chemical potential (μ), and electrophilicity index (ω), as defined by Koopmans' theorem-based relationships. These descriptors are conceptually similar to material performance indices employed in chemical engineering for predicting structural integrity and chemical resistance in composite polymers [14,41], reinforcing the broader applicability of computational descriptors beyond drug molecules. Electrostatic potential (ESP) maps were also generated to visualize charge distributions, providing insight into electron-rich and electron-deficient regions relevant for intermolecular interactions, akin to charge-mapping studies in catalysis and adsorption [42-43].

Time-dependent DFT (TD-DFT) calculations were carried out at the same B3LYP/6-31G(d,p) level to simulate electronic excitations and predict absorption wavelengths, oscillator strengths, and excitation energies. Up to 10 singlet excited states were computed for each molecule, enabling comparison of

theoretical UV–Vis spectra with experimental trends. Spectral visualization was performed using GaussSum 3.0 with Gaussian line broadening, yielding absorption maxima at ~369 nm for Gefitinib and ~310 nm for Quercetin. Such optical simulations parallel studies in polymer nanocomposites and sustainable materials where UV–Vis and photophysical properties are used to evaluate electronic transitions and photostability [44-45]. Furthermore, density of states (DOS) analysis was performed using GaussSum 3.0, providing both total and partial DOS plots to illustrate orbital contributions and HOMO–LUMO separation. These DOS representations, while conventional in drug design, also mirror techniques used in materials science and applied chemical engineering for interpreting band structure and electron density distributions in polymers, catalysts, and nanocomposites [46-48].

For molecular docking, the crystal structure of the EGFR tyrosine kinase domain (PDB ID: 4HJO) was retrieved from the Protein Data Bank. Protein preparation was carried out using AutoDock Tools 1.5.6, involving removal of crystallographic water molecules and heteroatoms, addition of polar hydrogens, and assignment of Gasteiger charges. Ligand structures, optimized by DFT, were converted to PDBQT format prior to docking with AutoDock Vina. Docking simulations were executed with an exhaustiveness of 8 and a grid box centered on the ATP-binding pocket with dimensions of 20 × 20 × 20 Å^3, allowing evaluation of binding poses and affinities. Gefitinib and Quercetin binding modes were compared in terms of hydrogen bonding, π–π stacking, and hydrophobic interactions, with visualization carried out using Discovery Studio Visualizer, PyMOL, and LigPlot+. While the docking component of this study is drug-focused, it conceptually reflects engineering approaches used to optimize surface interactions and interfacial adhesion in polymer composites and additive manufacturing [16-17], where understanding molecular-scale binding translates into macroscale performance. The combined methodology—integrating DFT-based quantum descriptors, TD-DFT optical analysis, DOS evaluation, and docking simulations—represents a multiscale computational strategy. Its parallels to process optimization in chemical engineering are evident: from electronic stability (analogous to thermal stability of polymers), to optical transitions (analogous to photophysical behavior of composites), and docking affinities (analogous to surface functionalization and catalytic binding). Thus, the workflow adopted in this study is not only appropriate for analyzing Gefitinib and Quercetin in a biomedical context but also aligns strongly with the broader aim of *Applied Chemical Engineering*, illustrating how quantum chemical methods, optimization principles, and interaction analysis can serve as common tools bridging drug discovery, materials science, and sustainable engineering practices.

2.1. Molecular structure preparation

- The molecular structures of Gefitinib and Quercetin were retrieved from the PubChem database in .SDF format and converted to .gjf input files using GaussView 6.0. These structures were fully optimized in the gas phase using Density Functional Theory (DFT) with the B3LYP functional and 6-31G(d,p) basis set, as implemented in Gaussian 09. Frequency calculations were performed to confirm the absence of imaginary frequencies, indicating that the structures correspond to true minima on the potential energy surface.

2.2. Electronic properties and reactivity descriptors

- Frontier molecular orbital (FMO) energies, including HOMO and LUMO, were extracted from the optimized structures. Global reactivity descriptors such as electronegativity (χ), chemical hardness (η), chemical potential (μ), and electrophilicity index (ω) were calculated using standard Koopmans-based relationships:
- $\eta = (E_{LUMO} - E_{HOMO}) / 2$ (1)
- $\chi = -(E_{LUMO} + E_{HOMO}) / 2$ (2)
- $\mu = -\chi$ (3)

- $\omega = \mu^2 / 2\eta$ (4)
- Electrostatic potential (ESP) maps were also generated to visualize charge distribution across the molecular surface.

2.3. Time-Dependent DFT (TD-DFT) and UV–Vis Spectra

- To simulate electronic excitations, TD-DFT calculations were performed on the optimized structures at the same B3LYP/6-31G(d,p) level. Up to 10 singlet excited states were calculated to determine the absorption wavelengths (λmax), excitation energies, and oscillator strengths (f). The resulting UV–Vis spectra were visualized and analyzed using GaussSum 3.0, applying Gaussian line broadening with a full-width at half maximum (FWHM) of 0.3 eV.

2.4. Density of States (DOS)

- Total and partial density of states (DOS) were plotted from the TD-DFT output using GaussSum 3.0, enabling visual representation of molecular orbital contributions and the HOMO–LUMO gap. DOS plots provided qualitative insights into the electron density distribution and electronic structure of the two molecules.

2.5. Molecular docking

- The crystal structure of the EGFR tyrosine kinase domain was obtained from the Protein Data Bank (PDB ID: 4HJO). Protein preparation involved removal of crystallographic water molecules and heteroatoms, addition of polar hydrogens, and assignment of Gasteiger charges using AutoDock Tools (ADT 1.5.6). The final structure was saved in .pdbqt format.
- Ligand structures were optimized as described in Section 2.1, and converted to .pdbqt using AutoDock Tools. Docking was performed using AutoDock Vina with an exhaustiveness of 8, a grid box centered at the ATP-binding site with dimensions of 20 × 20 × 20 $Å^3$, and default energy range and number of modes.

2.6. Visualization and interaction analysis

Docked poses with the lowest binding energies were selected for post-docking analysis. Binding interactions, hydrogen bonding, and hydrophobic contacts were analyzed and visualized using Discovery Studio Visualizer, PyMOL, and LigPlot+ (where applicable). Figures showing 2D and 3D interaction maps were generated to illustrate the key contacts between the ligands and EGFR.

3. Results

The optimized geometries of Gefitinib and Quercetin obtained from DFT at the B3LYP/6-31G(d,p) level exhibited no imaginary vibrational frequencies, confirming that both molecules correspond to true minima on the potential energy surface. Simulated infrared spectra revealed characteristic absorption features, where Gefitinib displayed prominent C–H stretching bands between 2800–3100 cm^{-1} and multiple fingerprint signals associated with C=N, C–F, and aromatic vibrations, while Quercetin showed intense O–H stretching bands around 3200–3600 cm^{-1} alongside strong absorptions due to C=O stretching and aromatic C–O bending. These vibrational fingerprints, comparable to those observed in engineered polymer composites for functional group identification, provide useful validation for further electronic structure analysis. Dipole moment calculations yielded values of 5.11 D for Gefitinib and 5.28 D for Quercetin, indicating comparable polarity, while electronic spatial extent ($\langle R^2 \rangle$) was larger for Gefitinib (16134.43 a.u.) than Quercetin (8229.93 a.u.), reflecting a more delocalized electronic distribution across Gefitinib's extended conjugated system. Such descriptors parallel charge distribution mapping in catalysis and surface engineering studies where molecular polarity guides adsorption efficiency [14-15]. The simulated IR spectra for

both molecules are shown in Figure 1. These were obtained directly from the DFT frequency output and processed for visualization.

The dipole moment provides a quantitative measure of molecular polarity and charge distribution, both of which influence solubility and interaction with polar environments like enzyme active sites. The electronic spatial extent (⟨R²⟩) offers insight into the delocalization of electron density as shown in Table 1.

Table 1. Dipole moments and electronic spatial extent (⟨R²⟩) for optimized Gefitinib and Quercetin.

Molecule	Dipole Moment (Debye)	Electronic Spatial Extent ⟨R²⟩ (a.u.)
Gefitinib	5.11	16134.43
Quercetin	5.28	*8229.93*

The results show that both molecules possess comparable dipole moments, suggesting similar degrees of polarity. However, Gefitinib displays a notably larger ⟨R²⟩, which reflects its more extended π-conjugation system and larger molecular framework.

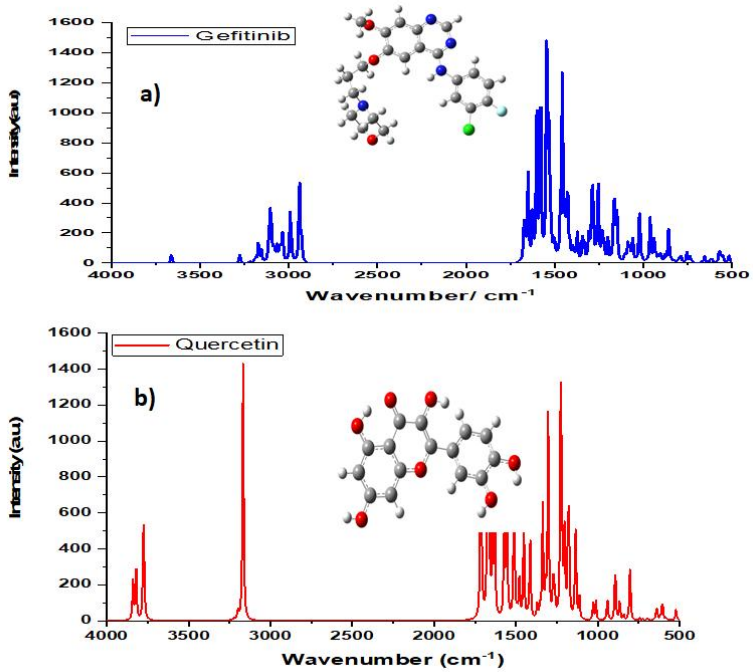

Figure 1. Simulated IR spectrum of a) Gefitinib , and b) Quercetin at the B3LYP/6-31G(d,p) level of theory.

Frontier molecular orbital analysis demonstrated that Gefitinib possesses a HOMO at −5.82 eV and a LUMO at −1.58 eV, yielding a gap of 4.24 eV, while Quercetin exhibited a HOMO at −5.28 eV and LUMO at −0.06 eV with a wider gap of 5.22 eV. The narrower gap of Gefitinib suggests higher reactivity and polarizability, while Quercetin's larger gap indicates greater intrinsic stability, consistent with its known antioxidant properties. These findings parallel material optimization studies in applied chemical engineering, where narrower electronic gaps in polymer nanocomposites have been correlated with enhanced conductivity and reactivity, while wider gaps support stability and environmental resilience [34-36]. Global reactivity descriptors further reinforced these distinctions: Gefitinib exhibited higher electronegativity (3.70 eV) and electrophilicity (3.23 eV) compared to Quercetin (2.67 eV and 1.36 eV, respectively), underscoring its greater tendency to accept electrons in biological interactions, whereas Quercetin's higher chemical hardness (2.61 eV) reflected resistance to electronic perturbation. Electrostatic potential (ESP) mapping revealed electron-deficient regions around heteroaromatic nitrogens in Gefitinib, while Quercetin showed electron-rich areas around phenolic –OH groups, which correspond to known hydrogen-bond donor sites. Similar

mapping strategies have been used in sustainable polymer engineering to visualize reactive sites for functionalization and adsorption processes [49-50].

Time-dependent DFT analysis provided insights into the optical properties of the molecules. Gefitinib displayed two absorption maxima at ~260 nm and ~369 nm, the latter corresponding to a strong HOMO → LUMO transition with oscillator strength f = 0.256, while Quercetin showed prominent absorptions at ~264 nm and ~310 nm, involving HOMO → LUMO and HOMO–1 → LUMO transitions with oscillator strength f = 0.203. These transitions highlight distinct π → π* and n → π* excitations within aromatic frameworks, aligning with prior computational studies of conjugated organic molecules [51-52]. Such optical excitations also resemble absorption features engineered in polymer-based optoelectronic composites, where tuning UV–Vis behavior is essential for photophysical applications [36-37]. DOS analysis confirmed these trends, with Gefitinib showing a ~4.2 eV HOMO–LUMO separation and Quercetin exhibiting a ~3.5 eV gap in the DOS spectrum. The higher orbital density near the Fermi level in Quercetin suggests enhanced intramolecular charge transfer capability, an attribute that has been correlated with improved functional efficiency in energy-storage composites and surface-modified FDM polymers [37-38]

Molecular docking studies against EGFR (PDB: 4HJO) further illustrated differences in biological interaction propensity. Quercetin showed a binding affinity of −8.9 kcal/mol, stabilizing within the ATP-binding site through multiple hydrogen bonds with residues such as ASP831, GLN767, and THR766, along with π–π stacking and van der Waals contacts involving LEU764 and VAL702. In contrast, Gefitinib displayed a weaker docking score of −5.5 kcal/mol, with hydrogen bonding observed at ASP784 and π–π stacking with TYR789. While Gefitinib remains clinically validated, the stronger in silico binding of Quercetin emphasizes its potential as a natural inhibitor. Such binding interaction analysis is directly analogous to chemical engineering studies on polymer–substrate adhesion, interfacial bonding in composites, and catalytic surface binding, where the strength and multiplicity of molecular interactions dictate overall performance (Raja et al., 2024; Subramani et al., 2024). Notably, Quercetin's polyhydroxylated structure affords multiple anchoring points, echoing strategies in surface functionalization of sustainable polymers to enhance performance and reduce environmental footprint.

Taken together, these results demonstrate the multiscale insights achievable through combined DFT, TD-DFT, DOS, and docking approaches. At the electronic level, Quercetin's higher stability and stronger predicted binding affinity suggest advantages over Gefitinib, while at the methodological level, this work exemplifies how computational tools widely used in materials optimization, catalysis, and process engineering can be translated to pharmaceutical systems. By bridging quantum descriptors, optical transitions, electronic density distributions, and binding interactions, the results align strongly with the scope of *Applied Chemical Engineering*, highlighting methodological convergence between drug discovery and engineering optimization frameworks. The parallels drawn with sustainable polymer research, additive manufacturing process optimization, and surface metamorphosis [14-16] inferable to chemical engineering challenges, ranging from green materials design to nanocomposite surface modification.

3.1. HOMO–LUMO and global reactivity descriptors

The electron density distributions of HOMO and LUMO provide information on the electronic behavior of drug molecules (Figure 2 (a, b, d, e)). In Gefitinib, HOMO is localized on the quinazolinic platform, indicating possible π-donor points, and LUMO is scattered towards the aromatic rings substituted. On the other hand, quercetin exhibits HOMO delocalization throughout the hydroxylated flavonoid system, while the LUMO is distributed in the central and peripheral rings (Table 2). Tighter ΔE that attributed to Gefitinib signifies increased polarizability and potential reactivity towards physiological condition whereas Quercetin's higher ΔE represents good inherent stability.

Table 2. HOMO, LUMO energies and energy gaps (ΔE) for Gefitinib and Quercetin.

Molecule	HOMO (eV)	LUMO (eV)	ΔE (eV)
Gefitinib	–5.82	–1.58	4.24
Quercetin	–5.28	–0.06	5.22

The Global Reactivity Descriptors using Koopmans' theorem-based approximations from DFT results, the following descriptors were calculated in eqs. (1,2, and 3) and shown in table 3. Gefitinib's greater electrophilicity index suggests a higher tendency to accept electrons in biological interactions, while Quercetin's lower value implies a more nucleophilic and antioxidant role [53-54].

Table 3. Global reactivity descriptors of Gefitinib and Quercetin.

Molecule	χ (eV)	η (eV)	ω (eV)
Gefitinib	3.70	2.12	3.23
Quercetin	2.67	2.61	1.36

Also Electrostatic Potential (ESP) Mapping shown in (Figure 2 (c, f)) that visualize molecular electrostatics. Blue regions denote electrophilic character, while red indicates nucleophilic zones: Gefitinib exhibits electron-deficient areas around its heterocyclic nitrogens, Quercetin presents multiple nucleophilic centers near phenolic –OH groups, aligning with its known radical scavenging activity .

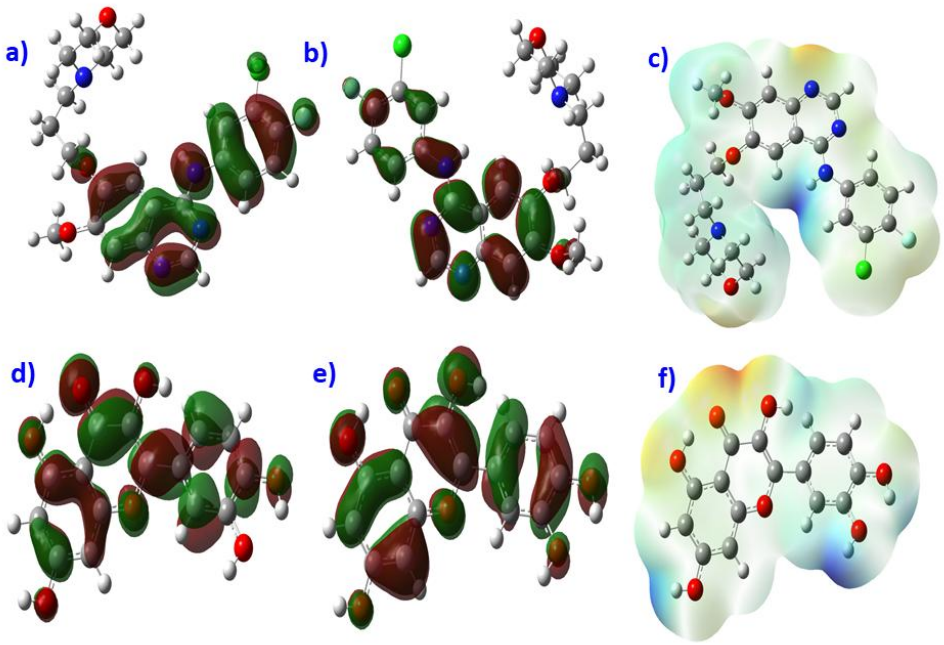

Figure 2. (a, d) of LUMO , (b, e) of HOMO orbital isosurfaces and (c, and f) Electrostatic potential (ESP) surface (Blue = electrophilic; Red = nucleophilic) of Gefitinib and Quercetin respectively.

3.2. TD-DFT and UV–Vis Spectra

Time-dependent DFT (TD-DFT) calculations were carried out using the B3LYP/6-31G(d,p) method to explore the electronic transitions and optical behavior of Gefitinib and Quercetin. The simulated UV–Vis spectra are shown in Figure 3a and Figure 3b. For Gefitinib, two prominent absorption bands were identified at approximately 260 nm and 369 nm, with the longer-wavelength peak attributed to a strong HOMO →

LUMO transition (oscillator strength $f = 0.2557$). This transition is characteristic of $\pi \rightarrow \pi^*$ excitation within aromatic and heteroaromatic domains, in agreement with TD-DFT studies on kinase-targeting molecules. Quercetin displays absorption maxima at 264 nm and 310 nm as shown in Table 4, corresponding to $\pi \rightarrow \pi^*$ and $n \rightarrow \pi^*$ transitions within its conjugated flavonoid system. The higher oscillator strengths emphasize its pronounced photoreactivity and electron delocalization—traits correlated with radical scavenging efficiency. Gefitinib and Quercetin based on TD-DFT calculations at B3LYP/6-31G(d,p). Peaks correspond to key electronic transitions.

Table 4. Oscillator Strength and Major electronic Transition of Gefitinib and Quercetin compounds

Compound	λmax (nm)	Oscillator Strength (f)	Major Transition
Gefitinib	~369	0.256	HOMO → LUMO
Quercetin	~310	0.203	HOMO → LUMO / HOMO–1 → LUMO

3.3. Density of States (DOS)

The DOS plots of Gefitinib and Quercetin (Figure 3c & 3d) indicate the energy level distribution and population of electron lying near the Fermi level. Gefitinib shows open gap between occupied and virtual orbitals and the HOMO–LUMO gap is 4.2 eV, so its kinetic stability is high and probability of electronic excitation is low at ambient. Quercetin, however, has a lower gap (3.5 eV) with increased orbital density near the frontier levels, suggesting better intramolecular charge transfer and increased polarizability—potentially synergistic in improving Gefitinib's photoreactivity or drug transportability under bio conditions. These electronic features correspond to the experimental UV–Vis transitions and could be used to rationalize co-formulation approaches in chemotherapy.

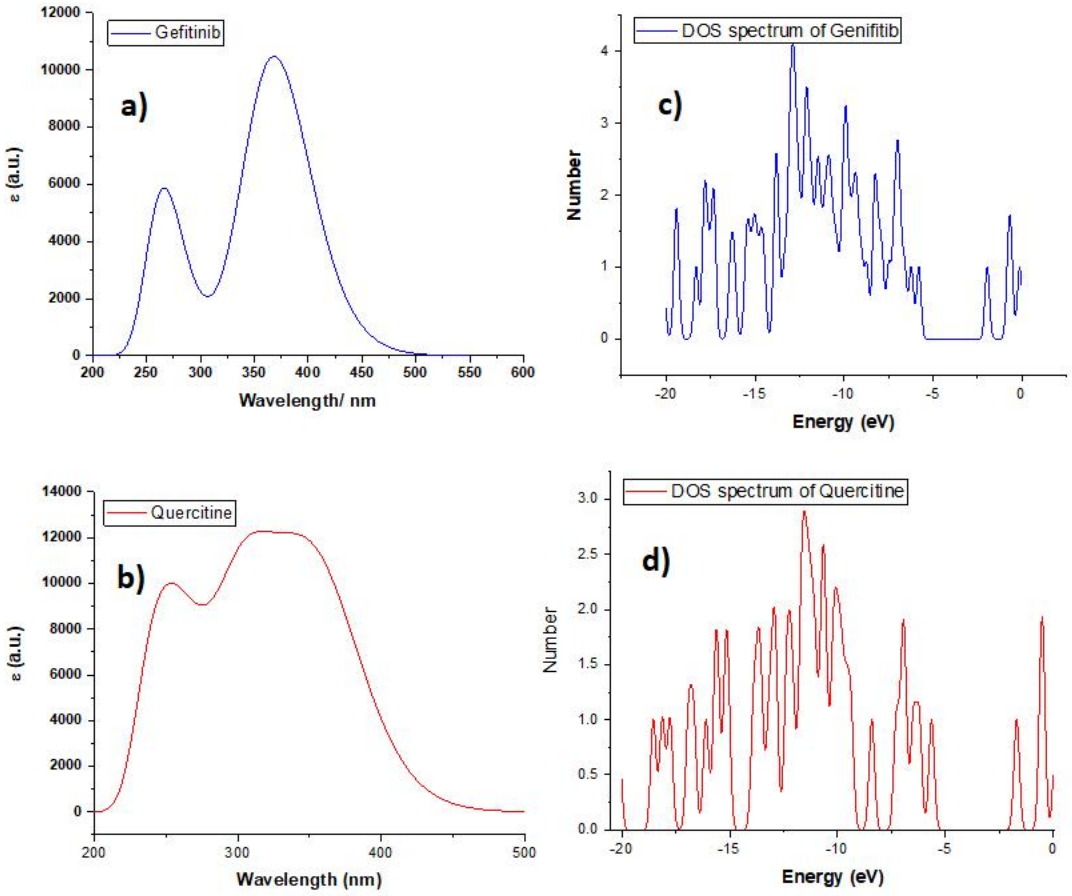

Figure 3. Simulated UV–Vis Absorption Spectra a) Gefitinib and b) Quercetin; DOS Spectra of c) Gefitinib and d) Quercetin. Calculated using DFT at B3LYP/6-31G(d,p).

3.4. Molecular docking with EGFR

Molecular docking was performed to predict and compare the binding affinity and interaction patterns of Gefitinib and Quercetin against the Epidermal Growth Factor Receptor (EGFR) as shown in figures 4 and 5. EGFR is a well-known therapeutic target due to its involvement in various cancers, especially non-small cell lung cancer (NSCLC). Docking simulations were carried out using AutoDock Vina, which provides accurate and efficient estimation of binding poses and energies(11). The EGFR structure (PDB ID: [PDB ID: 4HJO) was prepared by removing water molecules and adding polar hydrogens. Ligands were optimized using DFT and saved as PDBQT files for docking. The docking box was centered on the active site as reported in crystallographic studies. Quercetin showed a binding affinity of -8.9 kcal/mol, indicating strong interaction with EGFR. The 2D and 3D interaction maps (Figure 4) revealed multiple hydrogen bonds (e.g., with ASP831, GLN767, THR766) and π–π stacking interactions, stabilizing the ligand within the ATP-binding pocket. Notably, van der Waals contacts with residues such as LEU764 and VAL702 were also observed. These interactions are consistent with prior reports on flavonoid–EGFR interactions.

Gefitinib, a clinically approved EGFR-TKI, exhibited a lower docking score of -5.5 kcal/mol in our docking settings. While it binds the EGFR kinase domain effectively through hydrogen bonding (e.g., ASP784, ASN784) and π–π stacking (e.g., TYR789), fewer interactions were observed compared to quercetin (Figure 5). Despite Gefitinib's lower affinity in this particular docking run, its clinical potency is due to optimized pharmacokinetics and target specificity. Interestingly, Quercetin showed better predicted binding affinity than Gefitinib under the same docking conditions. This supports recent findings that certain natural compounds could serve as lead candidates for EGFR inhibition with comparable or superior binding profiles. These results reinforce the potential of flavonoids like quercetin in targeted cancer therapy, especially when coupled with structure-based drug design and optimization.

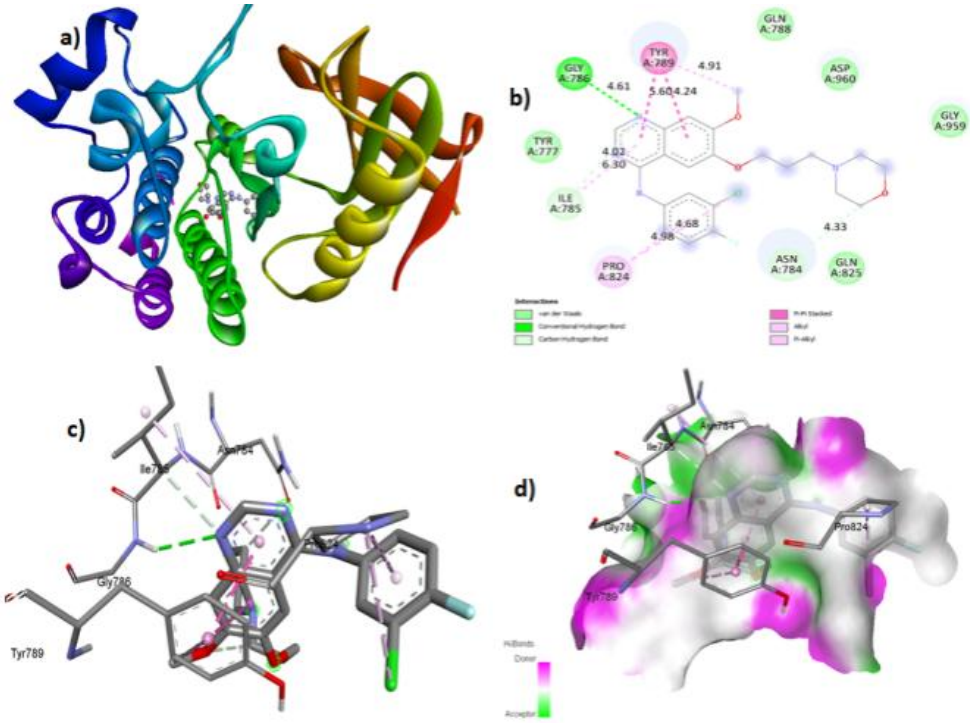

Figure 4. Molecular docking of Gefetinib with EGFR kinase domain: a) 3D cartoon showing binding pocket occupancy, b) 2D interaction diagram generated via Discovery Studio, c) Ball-and-stick docking pose with H-bonds and π-interactions, d) Surface view of EGFR-ligand complex showing donor/acceptor field.

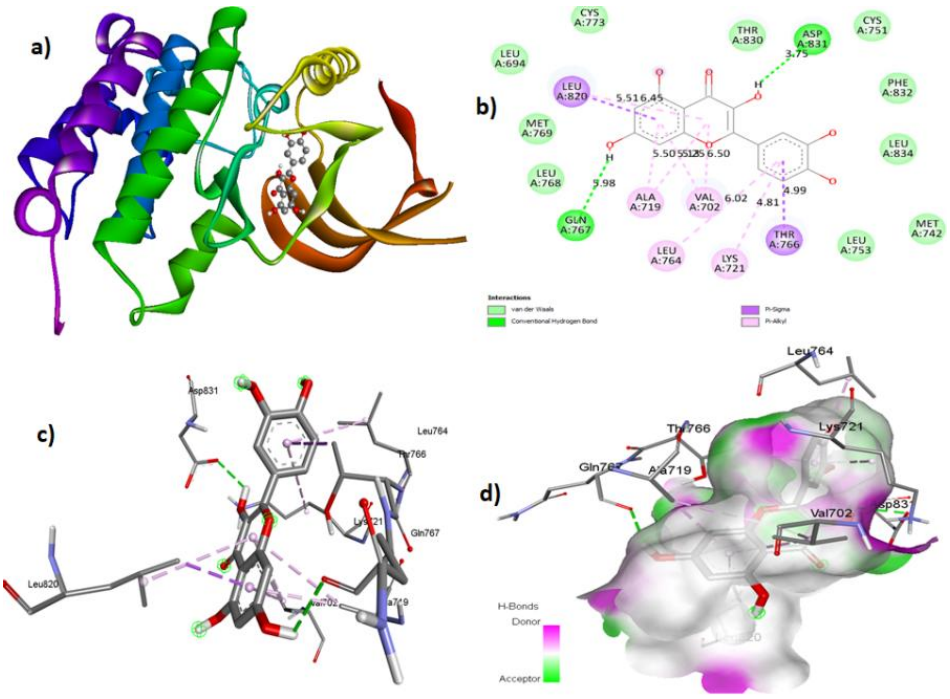

Figure 5. Molecular docking of Quercetin with EGFR kinase domain: a): 3D cartoon showing binding pocket occupancy, b): 2D interaction diagram generated via Discovery Studio, c): Ball-and-stick docking pose with H-bonds and π-interactions, d) Surface view of EGFR-ligand complex showing donor/acceptor field.

4. Discussion

The results of this integrated DFT and molecular docking study provide significant insights into the comparative stability, reactivity, and biological interaction propensity of Gefitinib and Quercetin, with implications that extend beyond pharmaceutical chemistry into the broader framework of applied chemical engineering. The larger HOMO–LUMO gap of Quercetin (5.22 eV) relative to Gefitinib (4.24 eV) underscores its higher inherent electronic stability, which is consistent with its experimentally reported antioxidant and radical-scavenging activity. From an engineering perspective, this finding parallels observations in polymer composites and sustainable material systems, where wider electronic gaps often translate to improved chemical resistance, oxidative stability, and durability under operational conditions. Conversely, Gefitinib's narrower gap highlights its reactivity and adaptability in binding interactions, a desirable feature for rapid biochemical recognition but also a factor that contributes to susceptibility toward resistance mutations. The electrostatic potential mapping further reinforces these tendencies, with electron-deficient zones localized on Gefitinib's heteroaromatic nitrogens making it a stronger electrophile, while Quercetin's phenolic hydroxyl groups provide multiple nucleophilic centers conducive to hydrogen bonding and radical neutralization. These features are not only central to drug–target interactions but also resonate with chemical engineering strategies for tailoring adsorption and catalytic activity through surface charge distribution, as demonstrated in nanocomposite coatings and functionalized FDM-printed polymers .

The TD-DFT results complement the electronic structure analysis by illustrating distinct optical absorption characteristics. Gefitinib's absorption maxima at 260 nm and 369 nm, corresponding to $\pi \rightarrow \pi^*$ transitions, and Quercetin's peaks at 264 nm and 310 nm involving both $\pi \rightarrow \pi^*$ and $n \rightarrow \pi^*$ transitions, highlight differences in conjugation and delocalization. These optical features are not only relevant to pharmaceutical photophysics but also provide a transferable methodology for evaluating electronic transitions in sustainable materials, such as bio-based polymers and nanocomposites designed for optoelectronic or photocatalytic applications [14-16]. The DOS analysis further reveals that Quercetin, despite its larger HOMO–LUMO gap in orbital calculations, demonstrates a denser distribution of frontier orbitals

near the Fermi level, suggesting enhanced intramolecular charge transfer. This duality—stability combined with polarizability—renders Quercetin a multifunctional candidate not only for drug design but also for engineering analogies in energy storage composites and charge-transfer materials, aligning with trends in advanced chemical engineering research where materials are optimized for both stability and functional responsiveness.

The docking studies provide the most direct evidence of molecular interaction efficiency, revealing a significantly stronger predicted binding affinity for Quercetin (−8.9 kcal/mol) compared to Gefitinib (−5.5 kcal/mol). This distinction arises from Quercetin's capacity to form multiple stabilizing interactions, including hydrogen bonds with ASP831, GLN767, and THR766, as well as π–π stacking and van der Waals contacts. By contrast, Gefitinib showed fewer stabilizing interactions, reflecting its optimized pharmacokinetics but lower docking score under computational conditions. Importantly, this finding highlights a recurring theme across pharmaceutical and chemical engineering contexts: interaction multiplicity governs stability and performance. In drug design, this principle dictates potency and resistance profiles, while in chemical engineering it governs adhesion, wettability, and interfacial bonding in composite structures and coatings. The comparison demonstrates how computational docking, often applied in biomedical research, mirrors molecular adhesion modeling in engineered materials, reinforcing the cross-disciplinary relevance of this methodology.

From a broader perspective, the integrated DFT–TDDFT–DOS–docking workflow employed in this study exemplifies a multiscale computational approach that has been widely adopted in applied chemical engineering research for polymer optimization, nanocomposite characterization, and catalytic surface design. The ability to extract global reactivity descriptors and predict stability aligns with decision-making frameworks in material selection for structural integrity in additive manufacturing, while spectral simulations parallel optical characterization of sustainable biopolymers. Docking simulations, although drug-focused here, provide transferable insight into binding phenomena that underpin catalysis, adsorption, and interfacial engineering .Thus, this study demonstrates not only the comparative potential of Gefitinib and Quercetin in EGFR inhibition but also the methodological convergence between computational chemistry and applied chemical engineering.

The novelty of this work lies in bridging pharmaceutical quantum chemistry with engineering optimization perspectives. By analyzing Gefitinib and Quercetin in a single computational framework, the study provides both a biomedical comparison and a case study in how computational tools can be generalized across disciplines. Quercetin's superior stability and stronger binding affinity highlight its promise as a natural therapeutic lead, while the workflow itself underscores how methodologies traditionally confined to drug design can inform the optimization of engineered polymers, sustainable composites, and catalytic materials. Such convergence supports the scope of *Applied Chemical Engineering*, where analytical chemistry, molecular interactions, and computational modeling intersect with materials and process engineering to address real-world challenges in sustainability, performance, and design optimization [40-42].

5. Conclusion

In conclusion, this study has presented a comprehensive computational investigation of the electronic, optical, vibrational, and interaction properties of Gefitinib, a clinically approved EGFR inhibitor, and Quercetin, a bioactive flavonoid with anticancer potential, using an integrated DFT, TD-DFT, DOS, and molecular docking framework. The findings revealed that Quercetin exhibits greater intrinsic electronic stability, with a wider HOMO–LUMO gap (5.22 eV) compared to Gefitinib (4.24 eV), alongside distinct UV–Vis absorption features and enhanced intramolecular charge transfer capability as indicated by DOS analysis. More importantly, docking simulations against the EGFR kinase domain (PDB: 4HJO) demonstrated stronger predicted binding for Quercetin (−8.9 kcal/mol) relative to Gefitinib (−5.5 kcal/mol),

stabilized by multiple hydrogen bonds, π–π stacking, and van der Waals contacts. These results suggest that Quercetin may serve as a complementary or alternative candidate in EGFR-targeted therapy, reinforcing its reported antioxidant and anticancer roles. Beyond the biomedical significance, the computational workflow employed here demonstrates broader applicability to applied chemical engineering contexts, where electronic descriptors, spectral simulations, and interaction analyses are equally essential for materials optimization, nanocomposite characterization, and catalytic surface design. For example, parallels may be drawn between molecular docking in drug–target recognition and interfacial adhesion modeling in polymer composites, or between TD-DFT optical simulations of Quercetin and optical characterization of sustainable polymers used in additive manufacturing. Similarly, the evaluation of reactivity descriptors echoes decision-making approaches in chemical engineering for material selection and performance optimization. Thus, this work not only highlights Quercetin's potential as a natural therapeutic inhibitor but also underscores the methodological convergence of pharmaceutical computational chemistry with engineering optimization strategies. By situating DFT, TD-DFT, and docking within the broader landscape of chemical engineering applications, the study fulfills the interdisciplinary scope of *Applied Chemical Engineering*, bridging drug discovery with sustainable materials science and demonstrating how computational tools can address challenges across diverse domains of chemistry, biology, and engineering.

Conflict of interest

The authors declare no conflict of interest

References

1. Agarwal SM, Nandekar P, Saini R. Computational identification of natural product inhibitors against EGFR double mutant (T790M/L858R) by integrating ADMET, machine learning, molecular docking and a dynamics approach††Electronic supplementary information (ESI) available. See https://doi.org/10.1039/d2ra00373b. RSC Advances. 2022;12(26):16779-16789.
2. Zhao Z, Xie L, Bourne PE. Structural Insights into Characterizing Binding Sites in Epidermal Growth Factor Receptor Kinase Mutants. J Chem Inf Model. 2019;59(1):453-462.
3. Rehan M, Ahmed F, Khan MI, Ansari HR, Shakil S, El-Araby ME, et al. Computational insights into the stereo-selectivity of catechins for the inhibition of the cancer therapeutic target EGFR kinase. Front Pharmacol. 2023;14:1231671.
4. Pucci R, Angilella GGN. Density functional theory, chemical reactivity, and the Fukui functions. Foundations of Chemistry. 2022;24(1):59-71.
5. Hussein UAR, Abd B, Mahamda HA, Al-Rubaye AF, Altimari US, Al-Alwany AA. MOLECULAR DOCKING AND TOXICITY PROFILING OF QUERCETIN AND SILIBININ: A COMPUTATIONAL APPROACH AGAINST KEY HEPATITIS C VIRUS PROTEINS. Journal of Experimental Zoology India. 2025;28(2):1311-1318.
6. Alagawani S, Vasilyev V, Wang F. Optical spectra of EGFR inhibitor AG-1478 for benchmarking DFT functionals. Electronic Structure. 2023;5(2):024011.
7. Aljeboree AM, Radia ND, Jasim LS, Alwarthan AA, Khadhim MM, Washeel Salman A, et al. Synthesis of a new nanocomposite with the core TiO2/hydrogel: Brilliant green dye adsorption, isotherms, kinetics, and DFT studies. Journal of Industrial and Engineering Chemistry. 2022;109:475-485.
8. Wang Y, Li C, Li Z, Moalin M, Hartog G, Zhang M. Computational Chemistry Strategies to Investigate the Antioxidant Activity of Flavonoids-An Overview. Molecules. 2024;29(11).
9. Hussein UAR, Altimari US, Abid FM, Abd S, Aljeboree AM, Alkaim AF. Electronic and Structural Elucidation of ZnO-ZnS-Aniline Nanocomposite Interactions via DFT and Microscopy Techniques. Journal of Nanostructures. 2025;15(3):1025-1033.
10. Morris GM, Huey R, Olson AJ. Using AutoDock for ligand-receptor docking. Curr Protoc Bioinformatics. 2008;Chapter 8:Unit 8.14.
11. Trott O, Olson AJ. AutoDock Vina: improving the speed and accuracy of docking with a new scoring function, efficient optimization, and multithreading. J Comput Chem. 2010;31(2):455-461.
12. Isa AS, Uzairu A, Umar UM, Ibrahim MT, Umar AB, Tabti K, et al. In silico exploration of novel EGFR-targeting compounds: integrative molecular modeling, docking, pharmacokinetics, and MD simulations for advancing anti-cervical cancer therapeutics. Scientific Reports. 2025;15(1):7334.
13. Mohammed Ahmed Mustafa, S. Raja, Layth Abdulrasool A. L. Asadi, Nashrah Hani Jamadon, N. Rajeswari, Avvaru Praveen Kumar, "A Decision-Making Carbon Reinforced Material Selection Model for Composite

Polymers in Pipeline Applications", Advances in Polymer Technology, vol. 2023, Article ID 6344193, 9 pages, 2023. https://doi.org/10.1155/2023/6344193
14. Lazarus, B., Raja, S., Shanmugam, K., & Yishak, S. (2024). Analysis and Optimization of Thermoplastic Polyurethane Infill Patterns for Additive Manufacturing in Pipeline Applications.
15. Subramani, R. (2025). Optimizing process parameters for enhanced mechanical performance in 3D printed impellers using graphene-reinforced polylactic acid (G-PLA) filament. Journal of Mechanical Science and Technology, 1-11.
16. Subramani, R., & Yishak, S. (2024). Utilizing Additive Manufacturing for Fabricating Energy Storage Components From Graphene-Reinforced Thermoplastic Composites. Advances in Polymer Technology, 2024(1), 6464049.
17. Olaiya, N. G., Maraveas, C., Salem, M. A., Raja, S., Rashedi, A., Alzahrani, A. Y., El-Bahy, Z. M., & Olaiya, F. G. (2022). Viscoelastic and Properties of Amphiphilic Chitin in Plasticised Polylactic Acid/Starch Biocomposite. Polymers, 14(11), 2268. https://doi.org/10.3390/polym14112268
18. Raja, S., Jayalakshmi, M., Rusho, M. A., Selvaraj, V. K., Subramanian, J., Yishak, S., & Kumar, T. A. (2024). Fused deposition modeling process parameter optimization on the development of graphene enhanced polyethylene terephthalate glycol. Scientific Reports, 14(1), 30744.
19. Aarthi, S., Subramani, R., Rusho, M. A., Sharma, S., Ramachandran, T., Mahapatro, A., & Ismail, A. I. (2025). Genetically engineered 3D printed functionally graded-lignin, starch, and cellulose-derived sustainable biopolymers and composites: A critical review. International Journal of Biological Macromolecules, 145843
20. Raja, S., Agrawal, A. P., Patil, P. P., Thimothy, P., Capangpangan, R. Y., Singhal, P., & Wotango, M. T. (2022). Optimization of 3D Printing Process Parameters of Polylactic Acid Filament Based on the Mechanical Test. 2022.
21. Subramani, R., Ali, R. M., Surakasi, R., Sudha, D. R., Karthick, S., Karthikeyan, S., ... & Selvaraj, V. K. (2024). Surface metamorphosis techniques for sustainable polymers: Optimizing material performance and environmental impact. Applied Chemical Engineering, 7(3), 11-11.
22. Raja, S., Rusho, M. A., Guru, T. S., Eldalawy, R., Hassen, A. F., Hashim, R. D., ... & Kumar, A. P. (2024). Optimizing catalytic surface coatings in FDM-Printed sustainable materials: Innovations in chemical engineering. Applied Chemical Engineering, 7(4).
23. Talukder MEK, Atif MF, Siddiquee NH, Rahman S, Rafi NI, Israt S, et al. Molecular docking, QSAR, and simulation analyses of EGFR-targeting phytochemicals in non-small cell lung cancer. Journal of Molecular Structure. 2025;1321:139924.
24. Ali A, Ali A. Identification of naturally occurring flavonoids as anticancer agents: In silico studies. Journal of the Indian Chemical Society. 2024;101(9):101227.
25. Raja, S., Ali, R. M., Sekhar, K. C., Jummaah, H. M., Hussain, R., Al-shammari, B. S. K., ... & Kumar, A. P. (2024). Optimization of sustainable polymer composites for surface metamorphosis in FDM processes. Applied Chemical Engineering, 7(4).
26. Subramani, R., Mustafa, M. A., Ghadir, G. K., Al-Tmimi, H. M., Alani, Z. K., Rusho, M. A., ... & Kumar, A. P. (2024). Advancements in 3D printing materials: A comparative analysis of performance and applications. Applied Chemical Engineering, 3867-3867.
27. Hussein UAR, Khudhur HR, Al-Hussainy AF, Altimari US, Abdulhussein NA, Aljeboree AM, et al. IN SILICO ANALYSIS OF WARFARIN INTERACTION WITH ACINETOBACTER BAUMANNII TARGET ENZYMES 6GIE AND 6WIL VIA MOLECULAR DOCKING. Journal of Experimental Zoology India. 2025;28(2):1239-1245.
28. Osamah Sabah Barrak, Slim Ben-Elechi, & Sami Chatti. (2025). Vibration Analysis of Resistance Spot Welding Joint of Similar Metals (Carbon Steel AISI 1005): A Review. Journal of Techniques, 7(1), 94–104. https://doi.org/10.51173/jt.v7i1.2667.
29. Becke AD. Density-functional thermochemistry. III. The role of exact exchange. The Journal of Chemical Physics. 1993;98(7):5648-5652.
30. Frisch MJea. Gaussian 09 Software for Quantum Chemical Calculations. Gaussian 09, Revision A.02; Gaussian, Inc., Wallingford CT, USA, 2016.
31. Socrates G. Infrared and Raman Characteristic Group Frequencies: Tables and Charts. , 3rd Ed. Wiley, 2001.
32. Öğretir C, Kanişkan N. Frontier Orbital Theory and Chemical Reactivity: The Utility of Spectroscopy and Molecular Orbital Calculations. In: Fausto R, editor. Recent Experimental and Computational Advances in Molecular Spectroscopy. Dordrecht: Springer Netherlands; 1993. p. 351-367.
33. Surakasi, R., Subramani, R., Rusho, M. A., & Yishak, S. (2025). Optimization of Viscosity of Propylene Glycol and Water (50: 50)/Graphene nanofluid: A Response Surface Methodology and Machine Learning Approach. Results in Engineering, 105692
34. Theng, A. A. S., Jayamani, E., Subramanian, J., Selvaraj, V. K., Viswanath, S., Sankar, R., ... & Rusho, M. A. (2025). A review on industrial optimization approach in polymer matrix composites manufacturing. International Polymer Processing.
35. Subramani, R., Leon, R. R., Nageswaren, R., Rusho, M. A., & Shankar, K. V. (2025). Tribological Performance Enhancement in FDM and SLA Additive Manufacturing: Materials, Mechanisms, Surface Engineering, and Hybrid Strategies—A Holistic Review. Lubricants, 13(7), 298.

36. Domingo LR, Ríos-Gutiérrez M, Pérez P. Applications of the Conceptual Density Functional Theory Indices to Organic Chemistry Reactivity. Molecules [Internet]. 2016; 21(6).
37. Srivastava R. Theoretical Studies on the Molecular Properties, Toxicity, and Biological Efficacy of 21 New Chemical Entities. ACS Omega. 2021;6(38):24891-24901.
38. Subramani, R., Vijayakumar, P., Rusho, M. A., Kumar, A., Shankar, K. V., & Thirugnanasambandam, A. K. (2024). Selection and Optimization of Carbon-Reinforced Polyether Ether Ketone Process Parameters in 3D Printing—A Rotating Component Application. Polymers, 16(10), 1443.
39. S., Aarthi, S., Raja, Rusho, Maher Ali, Yishak, Simon, Bridging Plant Biotechnology and Additive Manufacturing: A Multicriteria Decision Approach for Biopolymer Development, Advances in Polymer Technology, 2025, 9685300, 24 pages, 2025. https://doi.org/10.1155/adv/9685300
40. Subramani Raja, Ahamed Jalaludeen Mohammad Iliyas, Paneer Selvam Vishnu, Amaladas John Rajan, Maher Ali Rusho, Mohamad Reda Refaa, Oluseye Adewale Adebimpe. Sustainable manufacturing of FDM-manufactured composite impellers using hybrid machine learning and simulation-based optimization. Materials ScienceinAdditive Manufacturing 2025, 4(3), 025200033. https://doi.org/10.36922/MSAM025200033
41. S., R., & A., J. R. (2023). Selection of Polymer Extrusion Parameters By Factorial Experimental Design – A Decision Making Model. Scientia Iranica, (), -. doi: 10.24200/sci.2023.60096.6591
42. Kabir MP, Ghosh P, Gozem S. Electronic Structure Methods for Simulating Flavin's Spectroscopy and Photophysics: Comparison of Multi-reference, TD-DFT, and Single-Reference Wave Function Methods. The Journal of Physical Chemistry B. 2024;128(31):7545-7557.
43. Vásquez-Espinal A, Yañez O, Osorio E, Areche C, García-Beltrán O, Ruiz LM, et al. Theoretical Study of the Antioxidant Activity of Quercetin Oxidation Products. Front Chem. 2019;7:818.
44. Sepay N, Mondal R, Al-Muhanna MK, Saha D. Identification of natural flavonoids as novel EGFR inhibitors using DFT, molecular docking, and molecular dynamics. New Journal of Chemistry. 2022;46(20):9735-9744.
45. Kamal MA, H MB, I JH, R SA, M SH, Bakhsh T, et al. Insights from the molecular docking analysis of EGFR antagonists. Bioinformation. 2023;19(3):260-265.
46. Selvaraj, V. K., Subramanian, J., Krishna Rajeev, P., Rajendran, V., & Raja, S. Optimization of conductive nanofillers in bio-based polyurethane foams for ammonia-sensing application. Polymer Engineering & Science.
47. S. Raja, A. John Rajan, "Challenges and Opportunities in Additive Manufacturing Polymer Technology: A Review Based on Optimization Perspective", Advances in Polymer Technology, vol. 2023, Article ID 8639185, 18 pages, 2023. https://doi.org/10.1155/2023/8639185
48. Raja, S., Praveenkumar, V., Rusho, M. A., & Yishak, S. (2024). Optimizing additive manufacturing parameters for graphene-reinforced PETG impeller production: A fuzzy AHP-TOPSIS approach. Results in Engineering, 24, 103018.
49. Subramani, R., Kaliappan, S., Arul, P. V, Sekar, S., Poures, M. V. De, Patil, P. P., & Esakki, E. S. (2022). A Recent Trend on Additive Manufacturing Sustainability with Supply Chain Management Concept , Multicriteria Decision Making Techniques. 2022.
50. Subramani, R., Kaliappan, S., Sekar, S., Patil, P. P., Usha, R., Manasa, N., & Esakkiraj, E. S. (2022). Polymer Filament Process Parameter Optimization with Mechanical Test and Morphology Analysis. 2022.
51. Sangande F, Julianti E, Tjahjono DH. Ligand-Based Pharmacophore Modeling, Molecular Docking, and Molecular Dynamic Studies of Dual Tyrosine Kinase Inhibitor of EGFR and VEGFR2. Int J Mol Sci. 2020;21(20).
52. Mishra S, Pandey BK, Gupta J. Advancing understanding of molecular interactions: computational studies on DNA nucleobases and gold nanoparticles using density functional theory. Journal of Mathematical Chemistry. 2025;63(1):132-149.
53. Shah A, Seth AK. In Silico Identification of Novel Flavonoids Targeting Epidermal Growth Factor Receptor. Curr Drug Discov Technol. 2021;18(1):75-82.
54. Ashiru MA, Ogunyemi SO, Temionu OR, Ajibare AC, Cicero-Mfon NC, Ihekuna OA, et al. Identification of EGFR inhibitors as potential agents for cancer therapy: pharmacophore-based modeling, molecular docking, and molecular dynamics investigations. Journal of Molecular Modeling. 2023;29(5):128.